

Time-lapse nondestructive assessment of shock wave damage to kidney stones *in vitro* using micro-computed tomography^{a)}

Robin O. Cleveland^{b)}

Department of Aerospace and Mechanical Engineering, Boston University, 110 Cummington Street, Boston, Massachusetts 02215

James A. McAteer

Department of Anatomy and Cell Biology, Indiana University School of Medicine, 635 Barnhill Drive, Indianapolis, Indiana 46202

Ralph Müller^{c)}

Orthopedic Biomechanics Laboratory, Beth Israel Deaconess Medical Center and Harvard Medical School, 330 Brookline Avenue, Boston, Massachusetts 02215

(Received 27 March 2001; accepted for publication 14 July 2001)

To better understand how lithotripter shock waves break kidney stones, we treated human calcium oxalate monohydrate (COM) kidney stones with shock waves from an electrohydraulic lithotripter and tracked the fragmentation of the stones using micro-computed tomography (μ CT). A desktop μ CT scanning system, with a nominal resolution of 17 μ m, was used to record scans of stones at 50-shock wave intervals. Each μ CT scan yielded a complete three-dimensional map of the internal structure of the kidney stone. The data were processed to produce either two- or three-dimensional time-lapse images that showed the progression of damage inside the stone and at the surface of the stone. The high quality and excellent resolution of these images made it possible to detect separate patterns of damage suggestive of failure by cavitation and by spall. Nondestructive assessment by μ CT holds promise as a means to determine the mechanisms of stone fragmentation in SWL *in vitro*.
© 2001 Acoustical Society of America. [DOI: 10.1121/1.1401742]

PACS numbers: 43.80.Gx [FD]

I. INTRODUCTION

Shock wave lithotripsy (SWL) was first introduced in 1980¹ and has subsequently revolutionized the treatment of kidney stones. Despite its predominance in the treatment of urinary calculi there is a growing recognition that shock waves (SWs) cause trauma to the kidney²⁻⁴ that can result in acute problems⁵ and can lead to long-term complications in some patient groups.⁶⁻⁸ We present an imaging technique that provides new information on the fragmentation of kidney stones *in vitro*, information that may lead to advances in SWL that reduce side-effects.

A number of mechanisms have been proposed by which lithotripsy shock waves may destroy kidney stones. These include: *Spall*: the compressive component of the shock wave reflects off the distal surface and the stone fails in tension.^{1,9,10} *Cavitation*: the tensile component of the shock wave makes small bubbles grow in the fluid surrounding the stone; the violent collapse of the bubbles acts principally on the proximal surface of the stone.^{9,11,12} *Squeezing*: as the shock wave propagates through the stone a differential stress between the stone and the fluid develops which leads to a bulging and splitting along the SW axis.¹³ *Superfocusing*:

reflections from curved surfaces or corners of the stone can interfere constructively to produce localized regions of high stress.¹⁴ *Fatigue*: microscopic flaws in the stone grow due to the tensile stress¹⁵ or shear stress¹⁶ induced by successive SWs until macroscopic cracks develop and the stone breaks. These mechanisms are dependent to variable extent on different components of the lithotripter pressure pulse¹⁷ and the material properties of kidney stones.¹⁸

There is limited agreement in the literature as to the role of the mechanisms discussed above in the fragmentation process of kidney stones. We suggest that examination of a kidney stone at frequent intervals during its exposure to SWs will reveal the role of the various mechanisms. To test this idea we used an emerging imaging technique, x-ray micro-computed tomography (μ CT), which allows for the nondestructive assessment of x-ray attenuating materials. In μ CT, focused beams of x-rays are passed through an object and the absorption measured by a detector on the opposite side. The object is rotated about an axis and computed tomography (CT) is used to determine a 2D absorption map through thin slices. Stacks of 2D slices are then used to provide a 3D reconstruction of the object. The principal advantage of μ CT is that it is nondestructive and therefore allows time-lapse measurements. We demonstrate that with μ CT it is possible to track the early progression of SW damage in human kidney stones and that the pattern of damage is dependent on experimental manipulation of the environment surrounding the stone.

^{a)}Published as Letter to the Editor

^{b)}Author to whom correspondence should be addressed; electronic mail: robinc@bu.edu

^{c)}Now at: Institute for Biomedical Engineering, ETH and University of Zürich, Moussonstrasse 18, 8044 Zürich, Switzerland.

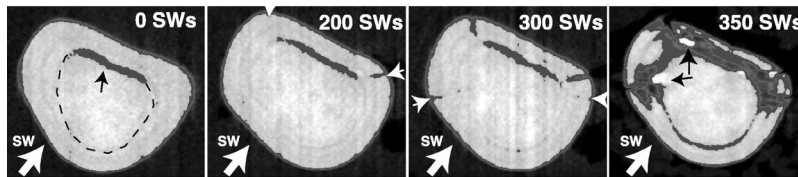


FIG. 1. Serial μ CT images of a COM stone "A1" at 0, 200, 300, and 350 SWs. Shock waves were incident from the lower left as indicated by the arrow. The black arrow in the baseline image denotes a region of low absorption that was in-line with a prominent lamella (dashed line). The gray color indicates regions of very low x-ray absorption. The small white arrows at 200 and 300 SWs denote the locations of new crack formation. By 300 SWs small gaps are visible along the lamellae and by 350 SWs the stone has separated into an outer shell and central core. The black arrows at 350 SWs indicate regions of high x-ray absorption.

II. MATERIALS AND METHODS

A. Kidney stones

Calcium oxalate mono-hydrate kidney stones (~ 4 mm diameter) were harvested from patients by percutaneous nephrostolithotomy (PCNL); COM is the most common stone formed in the body. At PCNL the stones were transferred directly into vials of sterile water for storage. Stone composition was determined by Beck Analytical Services (Indianapolis, IN) using microscopic visual inspection, qualitative chemical analysis, and infrared spectroscopy.

The stones were packaged so that they could be transported back and forth between the lithotripter (Indianapolis) and the μ CT facility (Boston) and could be re-positioned to their original spatial orientation within the lithotripter and the μ CT scanner. The stones were placed in polypropylene screw-cap cryovials (2 ml, 12×48 mm, Dot Scientific, Burton, MI) that were packed with water-saturated cotton gauze sponges (Johnson and Johnson, New Brunswick, NJ). In order to minimize transfer of air into the vial the gauze was soaked for 3 h in deionized water and kneaded by hand to displace bubbles. Gauze was inserted into the vials under water and packed tightly so that when a stone was put in and the cap secured, all under water, it would be held securely near the cap. One stone (stone A1) was packed entirely surrounded by gauze. This was done to reduce the opportunity for cavitation to take place at the surface of the stone. A second stone (stone A2) was loaded into a vial that had an optically clear, $0.1 \mu\text{m}$ thick, mylar window in the cap and was packed without gauze at its proximal surface. That is, the leading face of this stone was open to the surrounding water and was visible through the mylar window. Stone A1 was scanned by μ CT prior to treatment, and then scanned at 50 SW intervals until 350 SWs had been administered (8 μ CT scans performed). Stone A2 was treated until damage was visible through the mylar window (10 SWs). This stone was then scanned by μ CT.

B. Micro-computed tomography

A desktop μ CT imaging system (μ CT 20, Scanco Medical AG, Basserdorf, Switzerland) was used to image the stones. The system used a microfocus x-ray tube with a focal spot of $10 \mu\text{m}$ as an x-ray source. The filtered 40 kVp x-ray spectrum was peaked at 25 keV, allowing excellent stone-water contrast due to the pronounced photoelectric effect. The source produced a fan beam that was detected by a charge coupled device (CCD) array with 1024 elements.

Measurements were obtained by mounting the unprocessed specimen on a turntable that could be shifted automatically in the axial direction. Six hundred projections were taken over 216° (180° plus half the fan angle on either side). A standard convolution-back-projection procedure with a Shepp-Logan filter was used to reconstruct the CT images in 1024×1024 pixel matrices. The spatial resolution of the system was defined by the 10% contrast level in the modulation transfer function (MTF) resulting in a spatial resolution of $28 \mu\text{m}$.¹⁹

The vial that was used for shock wave treatment of the stone was placed directly inside the μ CT imaging device, that is, without disturbing the kidney stone. At each scan a total of 250 to 300 micro-tomographic slices, using a slice increment of $17 \mu\text{m}$, were acquired depending on the height of the sample (4.3 – 5.1 mm). The typical imaging time for a single scan of 300 slices was 8 h. Measurements were stored in three-dimensional image arrays with an isotropic voxel size of $17 \mu\text{m}$. A constrained three-dimensional Gaussian filter was used to partly suppress the noise in the volumes. Stone samples were segmented from background using a global thresholding procedure.²⁰ Because of the amount of data collected (of the order 1 GByte per 3D image of a stone) special visualization software was used that addresses the demands of rendering large triangulated objects including real-time functional animations.²¹

C. Shock wave lithotripsy

Shock wave exposures were performed using a research electrohydraulic lithotripter in which the acoustic output is equivalent to the Dornier HM3 lithotripter.²² The HM3 is the most widely used lithotripter in the US.²³ Vials were positioned with the stone at the focus of the lithotripter and the cap facing the SW source. The orientation of the vial ensured that SWs entered through the flat surface of the vial, which reduces artifacts associated with the interaction of the SW and the vial.²⁴ SWs were delivered at 20 kV and pulse rate of 1 Hz.

III. RESULTS

Figure 1 shows time-lapse μ CT images of a slice through the center of the stone A1 (gauze surrounded stone). Dark gray coloring was added during post-processing to regions of low absorption which we interpret to be associated with fractures or voids. The pre-SWL scan showed an internal region of low absorption in the form of a narrow band

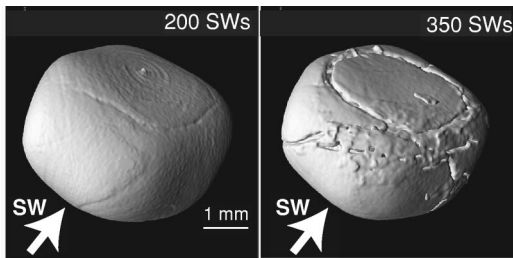


FIG. 2. Serial 3D surface rendered images of kidney stone A1 at 200 and 350 SWs. The formation of a circular chip at the distal side of the stone is consistent with failure by a spall mechanism.

near the distal side (relative to the SW source) of the stone. This region appeared to be in line with a prominent lamella that circumscribed the core of the stone. At 200 SWs and 300 SWs precursors of cracks were evident at both ends of this region, appearing to grow in from the surface of the stone. Also at 300 SWs small cracks had formed at midline on the right and the left. This is the location where squeezing and stress concentrations associated with curvature would be expected. In addition, at 300 SWs minute defects could be seen along the lamella previously observed in frame 0-SW. At 350 SWs growth of fractures along this lamella had separated the stone into an inner core and an outer shell. The growth of the cracks observed in these images consistent with a fatigue type of process. A broad chip had separated from the distal side of the stone. Loss of this piece is consistent with failure by spall. At 350 SWs there were also localized regions of very high x-ray absorption, as indicated by the presence of bright white spots.

Figure 2 shows two images formed using 3D surface rendering from the same measurement series. The 3D images clearly show the formation and separation of a cap at the distal surface. Figure 3 shows the 350 SW frame of Fig. 2 rotated approximately 180 deg and demonstrates that the SW-entry side of this stone (stone A1, surrounded by gauze) suffered no loss of material. After 350 SWs the stone was removed from the vial and was observed to have broken into *seven* main pieces which corresponded with the 3D μ CT image. These included the distal cap, a central core, and five pieces that made up the remainder of the outer shell.

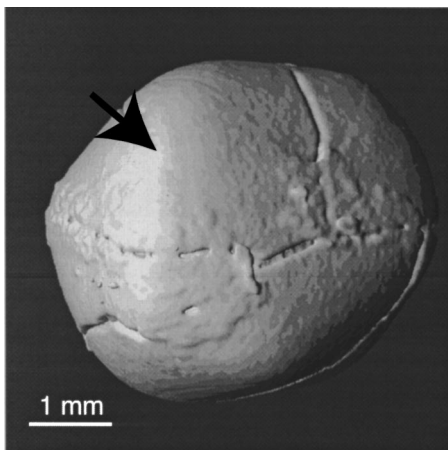


FIG. 3. Opposite side of stone A1 (Fig. 2, 350 SW). This image shows that the location of the SW entry, indicated by the arrow, has no sign of damage.

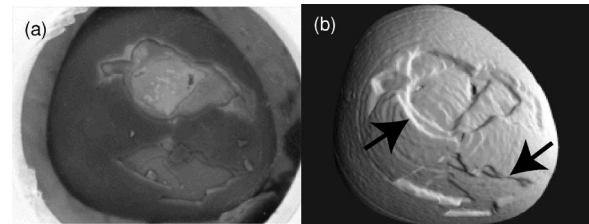


FIG. 4. Proximal surface of COM stone "A2" after 10 SWs. The upper frame is a surface rendering from μ CT data and shows that this surface has been chipped away, in contrast to Fig. 3. The lower frame shows an optical micrograph for comparison. The damage on this surface is consistent with a cavitation mechanism.

Figure 4 shows correlative μ CT and optical images of the proximal surface of stone A2 after 10 SWs. This face of the stone was open to the surrounding water, thus creating an environment that should allow cavitation to occur. Damage at this surface showed loss of broad, thin chips that revealed the lamellar substructure of the stone, in contrast to stone A1 which had no damage (Fig. 3). The μ CT scans (data not shown) indicated no other noticeable damage to the stone. Surface damage of this type is consistent with damage caused by cavitation in the surrounding fluid.

IV. DISCUSSION AND CONCLUSIONS

Our findings show for the first time that with μ CT it is possible to detect the initiation of micro-fractures within kidney stones treated by SWL. The resolution of the images was sufficient to reveal intrinsic structural features within the stones, such as concentric lamellae, and to nondestructively monitor the propagation of SW-induced cracks in relation to these landmarks. The long scan time (8 h/image) restricts the use of the technique to *in vitro* systems.

This demonstration involved only two stones. Thus it is premature to make any firm conclusions about the mechanisms that were involved in fragmentation. In this first test we chose to manipulate the environment surrounding the stones in order to alter cavitation. One stone (stone A2) was positioned with its proximal face open to the surrounding water, giving conditions that should be conducive to cavitation. This stone showed damage at its leading surface after only 10 SWs. Such damage *in vitro* seems comparable to the damage that occurs to target foils due to cavitation bubble collapse.²⁵

We packed the other stone (stone A1) tightly in water-saturated gauze in order to reduce the potential for cavitation to occur. This may not have eliminated cavitation altogether, but it is likely that gauze would interfere with bubble expansion, therefore, reducing the opportunity for effective bubble collapse.¹⁰ This stone showed essentially no damage at its proximal face, rather it suffered the loss of a large chip from its distal side. This is consistent with failure by spall. The μ CT images showed that cracks in this stone required hundreds of SWs to grow consistent with the idea that fatigue contributed to the failure. This stone also exhibited localized regions of high absorption and we speculate that the stone material may have been compacted in these regions, although the mechanism for the compaction is not clear.

In conclusion, we have demonstrated that μ CT imaging can reveal the internal structure of kidney stones and can be used to track the propagation of micro-fractures within the stone interior and at the stone surface. This preliminary test suggests that μ CT can detect patterns of SW-induced damage that are consistent with mechanisms of stone failure predicted by theory.

ACKNOWLEDGMENTS

The authors thank James Williams, Jr. for his suggestions during the preparation of this manuscript. This study has been partially supported by the National Institutes of Health through P01-DK-43881 (RC and JM) and the Maurice E. Müller Professorship in Bioengineering at Harvard Medical School (RM).

- ¹C. Chaussy, W. Brendel, and W. Schmiedt, "Extracorporeally induced destruction of kidney stones by shock waves," *Lancet* **2**, 1265–1268 (1980).
- ²J. V. Kaude, C. M. Williams, M. R. Millner, K. N. Scott, and B. Finlayson, "Renal morphology and function immediately after extracorporeal shock-wave lithotripsy," *Am. J. Roentgenol.* **145**, 305–313 (1985).
- ³J. E. Lingeman, J. Woods, P. D. Toth, A. P. Evan, and J. A. McAteer, "The role of lithotripsy and its side effects," *J. Urol. (Baltimore)* **141**, 793–797 (1989).
- ⁴A. P. Evan and J. A. McAteer, "Q-Effects of shock wave lithotripsy," in *Kidney Stones: Medical and Surgical Management*, edited by F. Coe, C. Pak, and G. M. Preminger (Raven, New York, 1996), pp. 549–570.
- ⁵A. P. Evan, L. R. Willis, J. E. Lingeman, and J. A. McAteer, "Renal trauma and the risk of long-term complications in shock wave lithotripsy," *Nephron* **78**, 1–8 (1998).
- ⁶A. K. Tuteja, J. P. Pulliam, T. H. Lehman, and L. W. Elzinga, "Anuric renal failure from massive bilateral renal hematoma following extracorporeal shock wave lithotripsy," *Urology* **50**, 606–608 (1997).
- ⁷D. A. Lifshitz, J. E. Lingeman, F. S. Zafar, D. H. Hollensbe, A. W. Nyhuis, and A. P. Evan, "Alterations in predicted growth rates of pediatric kidneys treated with extracorporeal shock wave lithotripsy," *J. Endourol* **12**, 469–475 (1998).
- ⁸G. Janetschek, F. Frauscher, R. Knapp, G. Hofle, R. Peschel, and G. Bartsch, "New onset hypertension after extracorporeal shock wave lithotripsy: Age related incidence and prediction by intrarenal resistive index," *J. Urol. (Baltimore)* **158**, 346–351 (1997).
- ⁹W. Sass, M. Braunlich, H. P. Dreyer, E. Matura, W. Folberth, H. G. Preismeyer, J. Seifert, "The mechanisms of stone disintegration by shock waves," *Ultrasound Med. Biol.* **17**, 239–243 (1991).
- ¹⁰Z. Ding and S. M. Gracewski, "Response of constrained and unconstrained bubbles to lithotripter shock wave pulses," *J. Acoust. Soc. Am.* **96**, 3636–3644 (1994).
- ¹¹L. A. Crum, "Cavitation microjets as a contributory mechanism for renal calculi disintegration in ESWL," *J. Urol. (Baltimore)* **140**, 1587–1590 (1988).
- ¹²M. Delius, W. Brendel, and G. Heine, "A mechanism of gallstone destruction by extracorporeal shock waves," *Naturwissenschaften* **75**, 200–201 (1988).
- ¹³W. Eisenmenger, "The mechanisms of stone fragmentation in ESWL," *Ultrasound Med. Biol.* **27**, 683–693 (2001).
- ¹⁴S. M. Gracewski, G. Dahake, Z. Ding, S. J. Burns, and E. C. Everbach, "Internal stress wave measurements in solids subjected to lithotripter pulses," *J. Acoust. Soc. Am.* **94**, 652–661 (1993).
- ¹⁵M. Lokhandwalla and B. Sturtevant, "Fracture mechanics model of stone comminution in ESWL and implications for tissue damage," *Phys. Med. Biol.* **45**, 1923–1940 (2000).
- ¹⁶X. Xi and P. Zhong, "Dynamic photoelastic study of the transient stress field in solids during shock wave lithotripsy," *J. Acoust. Soc. Am.* **109**, 1226–1239 (2001).
- ¹⁷A. J. Coleman and J. E. Saunders, "A survey of the acoustic output of commercial extracorporeal shock wave lithotripters," *Ultrasound Med. Biol.* **15**, 213–227 (1989).
- ¹⁸P. Zhong and G. M. Preminger, "Mechanisms of differing stone fragility in extracorporeal shock wave lithotripsy," *J. Endourology* **4**, 263–268 (1994).
- ¹⁹P. Rügsegger, B. Koller, and R. Müller, "A microtomographic system for the nondestructive evaluation of bone architecture," *Calcif. Tissue Int.* **58**, 24–29 (1996).
- ²⁰R. Müller and P. Rügsegger, "Micro-tomographic imaging for the non-destructive evaluation of trabecular bone architecture," *Studies in Health Technology and Informatics* **40**, 61–79 (1997).
- ²¹R. Müller, T. Hildebrand, and P. Rügsegger, "Noninvasive bone biopsy: A new method to analyze and display the three-dimensional structure of trabecular bone," *Phys. Med. Biol.* **39**, 145–164 (1994).
- ²²R. O. Cleveland, M. R. Bailey, N. Fineberg, B. Hartenbaum, M. Lokhandwalla, J. A. McAteer, and B. Sturtevant, "Design and characterization of a research electrohydraulic lithotripter patterned after the Dornier HM3," *Rev. Sci. Instrum.* **71**, 2514–2525 (2000).
- ²³J. E. Lingeman, "Extracorporeal shock wave lithotripsy devices: Are we making progress," in *New Developments in the Management of Urolithiasis*, edited by J. E. Lingeman and G. M. Preminger (Igaku-Shoin, New York, 1996), pp. 79–96.
- ²⁴R. O. Cleveland, J. A. McAteer, S. P. Andreoli, and L. A. Crum, "Effect of polypropylene vials on lithotripsy shock waves," *Ultrasound Med. Biol.* **23**, 939–952 (1997).
- ²⁵M. R. Bailey, D. T. Blackstock, R. O. Cleveland, and L. A. Crum, "Comparison of electrohydraulic lithotripters with rigid and pressure-release ellipsoidal reflectors: II. Cavitation fields," *J. Acoust. Soc. Am.* **106**, 1149–1160 (1999).